Protein Surface Charges and Ca²⁺ Binding to Individual Sites in Calbindin D9k: Stopped-Flow Studies

Stephen R. Martin,*,[‡] Sara Linse,[§] Charlotta Johansson,[§] Peter M. Bayley,[‡] and Sture Forsén[§]

Division of Physical Biochemistry, National Institute for Medical Research, Mill Hill, London NW7 1AA, England, and Physical Chemistry 2, Chemical Centre, P.O. Box 124, Lund University, S-221 00 Lund, Sweden

Received September 21, 1989; Revised Manuscript Received December 26, 1989

ABSTRACT: The kinetics of calcium dissociation from two groups of site-specific mutants of calbindin D9k—a protein in the calmodulin superfamily with two Ca²⁺ sites and a tertiary structure closely similar to that of the globular domains of troponin C and calmodulin—have been studied by stopped-flow kinetic methods, using the fluorescent calcium chelator Quin 2, and by ⁴³Ca NMR methods. The first group of mutants comprises all possible single, double, and triple neutralizations of three particular carboxylate groups (Glu-17, Asp-19, and Glu-26) that are located on the surface of the protein. These carboxylates are close to the two EF-hand calcium binding sites, but are not directly liganded to the Ca²⁺ ions. Conservative modification of these negative carboxylate side chains by conversion to the corresponding amides results in a marked reduction in the Ca²⁺ binding constants for both sites, as recently reported [Linse et al. (1988) *Nature 335*, 651–652]. The stopped-flow kinetic results show that this reduction in Ca²⁺ affinity derives primarily from a reduction in the Ca²⁺ association rate constant, k_{on}. The estimated maximum value of the association rate constant ($k_{on(max)}$) for Ca²⁺ binding to the wild-type protein is ca. 10^9 M⁻¹ s⁻¹. In contrast, for the mutant protein with three charges neutralized the maximum association rate constant is estimated to be only 2×10^7 M⁻¹ s⁻¹. In the presence of 0.1 M KCl, the value of $k_{on(max)}$ is only slightly affected in the case of the triple mutant but is substantially reduced in the case of the wild-type protein (to ca. 2×10^7 M⁻¹ s⁻¹). The second group of mutants involves amino acid substitutions and/or deletions in the Ca²⁺ binding loop of the N-terminal site. Although this site has a high affinity for Ca²⁺, it is unusual in that it contains two extra amino acids compared with an archetypal EF hand (such as that found at the C-terminal site). The alterations are aimed at making this N-terminal loop sequence more like that of an archetypal EF hand. Within this group of mutants are found examples of decreased rates of association and/or increased rate of dissociation for Ca²⁺ at the N-terminal site. In contrast, the modifications of the N-terminal site are found to have no significant effect on the kinetics of the C-terminal site.

O ne of the major aims of biophysical studies of proteins is the elucidation of the molecular events that underlie specific biological functions. The difficulty of this approach derives principally from the fact that the observed properties of a protein are the net result of interactions between a large number of different molecular groups. Furthermore, the physical nature of the interactions may vary from electrostatic to predominantly hydrophobic. Over the past few years the powerful molecular genetic technique of site-specific mutagenesis has had a major impact on structure–function studies of proteins. This technique has allowed detailed studies on the contribution of specific amino acid side chains to enzyme mechanisms (Shaw, 1987; Knowles, 1987) and of hydrophobic interactions to protein stability (Kellis et al., 1988; Matsumura et al., 1988). In addition—and of particular relevance to the present work—site-specific mutants have made possible an analysis of the influence of distant charges on pK_a values of histidines (Thomas et al., 1985) and also of charge effects on protein–protein interactions (Long et al., 1989; Weber et al., 1989), stability of proteins (Perry et al., 1989; Akke & Forsén, 1990) and isolated helices (Shoemaker et al., 1987; Sali et al., 1988), and ion transport (Clarke et al., 1989; MacKinnon et al., 1989).

In an attempt to explore the basic molecular mechanism of the Ca²⁺ binding process in the calmodulin family of reg-

ulatory proteins (Kretsinger, 1987), we have studied in some detail a number of mutants of recombinant bovine D9k (r-calbindin). This protein (M_r = 8500) has a tertiary structure very similar to that of one of the globular domains of calmodulin (Szebenyi & Moffat, 1986). It binds two Ca²⁺ ions with very high affinity ($K = 10^8$ M⁻¹; Linse et al. (1987) and shows positive cooperativity (Linse et al., 1987; Hofmann et al., 1988; Vogel et al., 1985). While the C-terminal Ca²⁺ site (site II) has the 12 amino acid sequence and general fold of an archetypal EF hand (Kretsinger, 1987; Kretsinger & Nockolds 1973), the N-terminal site (Site I) is unusual in that it contains a Ca²⁺ binding loop with two additional amino acids, one of which is a unique proline. The presence in calbindin D9k of only two Ca²⁺ binding sites facilitates the interpretation of kinetic and equilibrium data for Ca²⁺ binding and makes this protein an ideal choice for exploring the molecular basis of Ca²⁺ binding to single sites and of interactions between sites.

We have previously reported the effects on a number of equilibrium and kinetic properties of amino acid substitutions in and around site I (Linse et al., 1987, 1988; Forsén et al., 1988; Wendt et al., 1988). In the present work we report results on the dynamics of Ca²⁺ binding in two groups of mutant r-calbindins (see Table I). The aims of the present study were threefold:

(1) We studied the role of three specific carboxylate groups (Glu-17, Asp-19, and Glu-26) in the Ca²⁺ binding process. The crystal structure (Szebenyi & Moffat, 1986) shows that these carboxylate groups (see Figure 1) are not directly in-

*To whom correspondence should be addressed.
[‡] National Institute for Medical Research.
[§] Lund University.
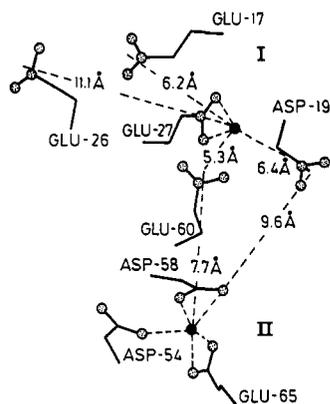
FIGURE 1: Cluster of negative surface residues around the two Ca^{2+} binding sites of calbindin D$_{9k}$. X-ray studies (Szebenyi & Moffat, 1986) show that only Glu-27, Asp-54, and Glu-65 are part of the inner ligand spheres of sites I and II. The distances between the Ca^{2+} ions (●) and the nonliganded carboxylate groups (midpoint between oxygens) are indicated.

volved as ligands but are situated on the protein surface near the Ca^{2+} sites, some 6–11 and 10–17 Å away from the cations of sites I and II, respectively. We have recently shown that neutralization of these negatively charged side chains, by substituting them with the corresponding amides, results in a marked lowering of the equilibrium Ca^{2+} binding constants (Linse et al., 1988). Here, we have used stopped-flow kinetic studies to establish to what extent this effect derives from either increased rates of Ca^{2+} dissociation or decreased rates of Ca^{2+} association.

(2) We explored the possibility that chosen alterations of the amino acid sequence of the pseudo EF hand (site I) would confer properties more like those of a typical calcium binding loop such as that of site II and investigated whether the consensus 12 amino acid sequence contains sufficient information to dictate the tertiary structure and general characteristics of the Ca^{2+} binding loop.

(3) We examined the effects of substitutions and/or deletions at one site on the kinetic properties of the other (unmodified) site and investigated the cooperativity between binding sites.

Here we report the results on the kinetics of Ca^{2+} binding in two groups of mutant r-calbindins (see Table I). Proteins in the first group (group A) contain all possible single, double, and triple neutralizations of the three surface carboxylates mentioned above. The second group (group B) involves substitutions and/or deletions in the atypical EF-hand Ca^{2+} binding loop of site I.

MATERIALS AND METHODS

Mutant proteins were produced in *Escherichia coli* by using synthetic genes (Brodin et al., 1986) and purified as described (Linse et al., 1987), except that the urea step was replaced by a heat denaturation step to avoid deamidation of the proteins (Chazin et al., 1989). Protein purity was checked by SDS–polyacrylamide and agarose gel electrophoresis, isoelectric focusing, and ¹H NMR.

The kinetic properties of wild-type calbindin and five mutant forms have been described elsewhere (Forsén et al., 1988). As noted previously (Forsén et al., 1988) the cited protein concentrations are based on weight and, owing to the presence of some residual water, are generally overestimated by some 10%.

All other chemicals were of reagent grade and were obtained from local suppliers. All solutions were prepared in a buffer containing 20 mM Pipes¹/KOH, pH 7.0, and were stored in

$$P \underset{}{\overset{K_1}{\rightleftharpoons}} PCa \underset{}{\overset{K_2}{\rightleftharpoons}} PCa_2$$
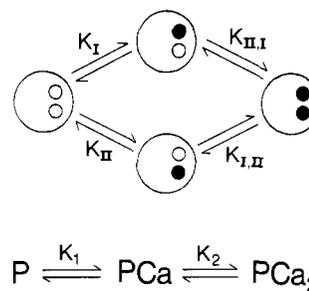
FIGURE 2: Definition of microscopic (or site) binding constants, K_I, K_{II}, $K_{I,II}$, and $K_{II,I}$, and the macroscopic (or stoichiometric) binding constants, K_1 and K_2. P represents the Ca^{2+}-free form of the protein, PCa a protein molecule with one Ca^{2+} ion bound (to either site I or II), and PCa$_2$ a protein molecule with both sites occupied. Free Ca^{2+} ions are omitted in the figure but are included in the expressions for the binding constants.

plastic containers. In studies of the effect of added KCl, all solutions were made 0.1 M in KCl.

Stopped-flow experiments were performed as described elsewhere (Forsén et al., 1988; Martin et al., 1985) with concentrations (before 1:1 stopped-flow mixing) of 30 μM calcium, 15 μM calbindin, and 200 μM Quin 2. Although this concentration of Quin 2 may not displace all the calcium from some mutants, it gave optimal signal to noise ratio in our stopped-flow system [see Forsén et al. (1988)].

Data analysis, involving fitting to one or two exponential functions, was performed as described previously (Forsén et al., 1988). Where necessary, we have corrected for interference from photobleaching of Quin 2 either by adding an additional very slow exponential to the fitting function or by incorporating a sloping base line in the fitting function. These methods gave virtually indistinguishable results. As before, a control experiment in which 15 μM calmodulin plus 60 μM calcium was mixed with 200 μM Quin 2 was used to calculate theoretical amplitudes for dissociation of Ca^{2+} from the calbindins (Forsén et al., 1988; Martin et al., 1985). Reaction amplitudes (A_s and A_f, where the subscripts refer to the slow and fast phases) are reported throughout in terms of the number of Ca^{2+} ions displaced. The rate constants k_f and k_s refer to the fast and slow dissociation processes, respectively, and the reported values are the average of at least eight individual measurements. A general scheme for binding of Ca^{2+} to calbindin D$_{9k}$ is shown in Figure 2. In this scheme, and throughout the text, the equilibrium constants are given as association constants. K_1 and K_2 are the macroscopic (stoichiometric) association constants; subscripts 1 and 2 refer to binding of the first and second Ca^{2+} ion, respectively. The microscopic (site) association constants are K_I (for binding at site I, site II empty), K_{II} (binding at site II, site I empty), $K_{I,II}$ (binding at site I, site II occupied), and $K_{II,I}$ (binding at site II, site I occupied).

^{43}Ca NMR spectra were obtained on a Nicolet 360 WB spectrometer at 24.34 MHz. A homemade horizontal probe with a solenoidal coil was used (Drakenberg et al., 1983). To minimize the effects of acoustic ringing, the RIDE sequence was used with a 90° pulse length of 40 μs. One thousand data points were recorded for a spectral width of ±10000 Hz. Up to 5 × 10⁶ transients were recorded during a total time of 15 h. The line shape of the ^{43}Ca NMR depends on the dissociation rate for the Ca^{2+} ion from the protein when this dissociation rate is in the intermediate range (10¹–10⁴ s⁻¹). To obtain the exchange rate at 25 °C, experimental and calculated

¹ Abbreviations: Quin 2, 2-[[2-[bis(carboxymethyl)amino]-5-methylphenoxy]methyl]-6-methoxy-8-[bis(carboxymethyl)amino]-quinoline; CaM, calmodulin; NMR, nuclear magnetic resonance; Pipes, piperazine-*N*,*N*′-bis[2-ethanesulfonic acid].

Table I: Macroscopic (Stoichiometric) Ca^{2+} Binding Constants (K_1 and K_2) for Wild-Type and Genetically Modified Calbindins [See Linse et al. (1988) and Johansson et al. (1990)][a]

protein	no KCl		0.10 M KCl	
	$\log K_1$	$\log K_2$	$\log K_1$	$\log K_2$
wild type	8.2	8.6	6.5	6.8
group A				
(E17Q)	7.4	8.1	6.3	6.5
(D19N)	7.6	8.0	6.5	6.2
(E26Q)	7.6 (0.3)	8.7 (0.3)	6.2	6.9
(E17Q + D19N)	7.4	7.1	6.5	5.7
(E17Q + E26Q)	6.8	7.8	6.2	6.3
(D19N + E26Q)	6.9	7.6	6.4	6.2
(E17Q + D19N + E26Q)	6.8	6.7	6.1	5.4
group B				
(P20Δ + A15Δ)	7.8	4.6		
(A15Δ + P20G)	8.0	4.3		
(A15Δ + P20G + N21Δ)	8.1	3.0		
(A15Δ)	7.7	6.3		

[a] Values refer to 25 °C, and uncertainties are usually 0.1 log unit unless otherwise indicated. We use the one-letter codes for amino acids in mutant definitions [see Creighton (1983)].

temperature dependencies of the line width at half-height were compared. The theoretical temperature dependence was calculated as described by Tsai et al. (1987).

RESULTS AND DISCUSSION

Macroscopic Ca^{2+} binding constants for the calbindin D_{9k} mutants are given in Table I. Although the data for the group A mutants have recently been published (Linse et al., 1988), some rather general comments can usefully be made here. The neutralization of negative surface charge residues has a very pronounced effect on the Ca^{2+} affinity of calbindin. In comparison with the wild-type protein, the Ca^{2+} affinity is gradually reduced as an increasing number of surface residues are neutralized. The effect appears to be additive within experimental error. The substantial reduction observed in K_1 (the first stoichiometric binding constant) and the fact that the

microscopic (site) binding constants are approximately the same in the wild-type protein (Linse et al., 1987) make it clear that both site binding constants K_I and K_{II} (note that $K_1 = K_I + K_{II}$) are greatly reduced by charge neutralization; thus, the group A mutations are clearly having a pronounced effect on the Ca^{2+} affinity at both sites.

Positive cooperativity is shown by all mutants in group A, and in some cases the degree of cooperativity is apparently greater than that shown in the case of the wild-type protein. In contrast, the mutants in group B appear to behave like a previously studied series of mutants in which Pro-20 was either deleted or replaced by a glycine (Linse et al., 1987; Forsén et al., 1988); i.e., the first stoichiometric binding constant (K_1) is similar to that for the wild type, and the second constant (K_2) is greatly reduced compared with that for the wild type. At first sight this suggests an interpretation similar to that used in previous studies [see, for example, Forsén et al. (1988)], i.e., that the modifications substantially reduce the affinity of Ca^{2+} for the modified site (I) while leaving the affinity of Ca^{2+} for site II largely unaltered.

For the group B mutants the observed kinetic behavior appears to the reasonably straightforward. Each mutant shows a slow dissociation process similar to that seen for the wild-type protein, ranging in rate from 1.5 s^{-1} for (A15Δ + P20G) up to 9.3 s^{-1} for (A15Δ + P20Δ) (see Table II). In each case this process clearly corresponds to the dissociation of a single Ca^{2+} ion. For the (A15Δ) mutant a second faster process is observed, and this also corresponds to the dissociation of a single Ca^{2+} ion, presumably from the modified site. For mutants (A15Δ + P20Δ), (A15Δ + P20G), and probably (A15Δ + P20G + N21Δ) the dissociation from the modified site is too fast to measure with the stopped-flow technique, but it has been measured by using ^{43}Ca NMR (Table III). The two methods complement each other in the sense that ^{43}Ca NMR cannot be used to determine dissociation rates slower than 10 s^{-1}. The value of k_s is generally increased by a factor of about 2 in the presence of added 0.1 M KCl for all four

Table II: Ca^{2+} Dissociation Rates (k) and Amplitudes (A) Obtained from Stopped-Flow Experiments on Genetically Modified Calbindins at 20 °C

protein	k_s (s^{-1})	$A_s{}^a$ (Ca^{2+})	k_f (s^{-1})	$A_f{}^a$ (Ca^{2+})
A (−KCl). (Experimental Conditions: 20 mM Pipes/KOH, pH 7.0)				
wild type	3.5 (0.5)	1.74 (0.28)		
(E17Q)	4.3 (0.8)	1.68 (0.18)		
(D19N)	8.3 (1.5)	0.82 (0.11)	21.5 (2.3)	0.69 (0.15)
(E26Q)	2.4 (0.6)	0.78 (0.23)	12.4 (4.2)	0.66 (0.14)
(E17Q + D19N)	6.3 (1.2)	0.43 (0.20)	15.3 (3.5)	0.79 (0.15)
(E17Q + E26Q)	3.9 (1.2)	0.73 (0.16)	18.3 (3.6)	0.83 (0.18)
(D19N + E26Q)	4.8 (1.3)	1.58 (0.22)		
(E17Q + D19N + E26Q)	3.4 (1.5)	1.02 (0.32)		
(A15Δ + P20Δ)	8.3 (1.5)	0.71 (0.13)		
(A15Δ + P20G)	1.5 (0.3)	0.83 (0.13)		
(A15Δ + P20G + N21Δ)	9.3 (2.5)	0.82 (0.15)	465 (285)	0.11 (0.17)
(A15Δ)	5.2 (0.9)	0.75 (0.19)	86.2 (12)	0.61 (0.13)
B (+KCl). [Experimental Conditions: Same as in (A) but with Buffer Made 0.1 M in KCl]				
wild type[b]	8.6 (1.5)	1.08 (0.18)	48.0 (7)	1.38 (0.29)
(E17Q)	11.0 (1.6)	0.95 (9.12)	100 (18)	0.52 (0.18)
(D19N)	12.5 (2.3)	0.75 (0.21)	48.6 (5.7)	0.65 (0.18)
(E26Q)	4.9 (1.2)	0.86 (0.19)	69.3 (12)	0.71 (0.22)
(E17Q + D19N)	8.5 (0.9)	0.51 (0.13)	22.7 (2.8)	0.93 (0.13)
(E17Q + E26Q)	8.7 (1.9)	0.87 (0.18)	132 (12)	0.69 (0.23)
(D19N + E26Q)	3.9 (1.8)	0.71 (0.12)	12.3 (2.5)	0.69 (0.22)
(E17Q + D19N + E26Q)	10.7 (3.8)	1.45 (0.45)		
(A15Δ + P20Δ)	16.5 (3.2)	0.86 (0.24)		
(A15Δ + P20G)	6.5 (0.8)	0.89 (0.09)		
(A15Δ + P20G + N21Δ)	22.6 (5.4)	0.90 (0.23)		
(A15Δ)	12.6 (2.3)	0.88 (0.22)	254 (24)	0.75 (0.18)

[a] Amplitudes are quoted as number of Ca^{2+} ions dissociating (see Materials and Methods). [b] The data for the wild-type protein and for (E17Q) in the presence of added KCl are taken from Forsén et al. (1988).

Table III: Ca²⁺ Dissociation Rates (k) Obtained from ⁴³Ca NMR Experiments on Genetically Modified Calbindins (See Figure 3)

protein	k (s⁻¹)
(D19N)	19
(E17Q + D19N + E26Q)	370
(A15Δ + P20Δ)	6000[a]
(A15Δ + P20G)	3000[a]
(A15Δ + P20G + N21Δ)	7500[a]
(A15Δ)	500[a]

[a] From Johansson et al. (1990).

FIGURE 3: Temperature dependence of the ⁴³Ca NMR line width for free Ca²⁺ in the presence of (O) (E17Q + D19N + E26Q) and (+) (D19N) calbindin mutants.

group B mutants. In the case of the (A15Δ) mutant, the presence of added KCl increases the value of k_f by a similar factor.

If we assume [see Forsén et al. (1988)] that dissociation of metal ions from the group B mutants occurs predominantly via the lower pathway of the scheme of Figure 2, we may derive estimates for the association rate constants for Ca²⁺ as follows. The macroscopic binding constants are related to the microscopic binding constants through

$$K_1 = K_I + K_{II} \qquad K_2 = K_{I,II}(K_{II}/K_I) \qquad (1)$$

From these equations (with $K_1 \gg K_2$ and by assuming sequential binding of Ca²⁺ [see Forsén et al. (1988)]) it follows that $K_1 = K_{II}$ and $K_2 = K_{I,II}$. Then, as $K_{I,II} = k_{on}^{I,II}/k_{off}^{I,II}$ (with $k_{off}^{I,II} = k_f$) and $K_{II} = k_{on}^{II}/k_{off}^{II}$ (with $k_{off}^{II} = k_s$) the values of $k_{on}^{I,II}$ and k_{on}^{II} may be calculated. If we include the ⁴³Ca NMR data for k_f values, then, with one exception, all the k_{on} values for the group B mutants lie in the range 0.6–8.1 × 10⁸ M⁻¹ s⁻¹. The exception is $k_{on}^{I,II}$ for the (A15Δ + P20G + N21Δ) mutant, for which we calculate a value of 7 × 10⁶ M⁻¹ s⁻¹. The structural consequences of the modifications contained in this mutant are not well understood at present. However, time-resolved fluorescence depolarization studies (Rigler et al., 1990) show an increased mobility for the Tyr-13 side chain in this mutant as compared with the wild-type protein.

For the group A mutants the observed stopped-flow kinetic behavior is again reasonably straightforward. With the exception of (E17Q) and (D19N + E26Q) these proteins show two clearly resolvable kinetic processes, each of which appears to correspond to the dissociation of only a single Ca²⁺ ion. The rate of the slow process varies from 2.4 s⁻¹ for (E26Q) to 8.3 s⁻¹ for (D19N), while the rate of the fast process ranges from 12.4 s⁻¹ for (E26Q) to 21.5 s⁻¹ for (D19N). The (D19N + E26Q) mutant shows only a single process with a rate of 4.8 s⁻¹, but this appears, from inspection of the reaction amplitude, to correspond to the dissociation of two Ca²⁺ ions; this interpretation is supported by the fact that two clearly resolvable processes are observed for experiments performed in the presence of 0.1 M KCl [see Table II and Forsén et al. (1988)]. The effects of neutralization of individual charges on dissociation rates thus appear to be nonadditive. The complementary nature of stopped-flow and ⁴³Ca NMR is shown by the data for the triple mutant (E17Q + D19N + E26Q); this mutant shows two processes with rates of 4.5 (slow process: stopped-flow, Table II) and 370 s⁻¹ [fast process: ⁴³Ca NMR, Table III; ⁴³Ca NMR data for (E17Q + D19N + E26Q) and (D19N) are shown in Figure 3]. The effect of added KCl for this group of mutants is generally rather similar to that observed for those in group B. The value of k_s is increased by up to a factor of 2, while the effect on k_f is more variable and is rather large in some cases [particularly for (E26Q) and (E17Q + E26Q)].

For these group A proteins (as well as for the wild-type protein) the interpretation of the kinetic data in terms of k_{on} values is not straightforward because the equilibrium constant data show that Ca²⁺ binding is not sequential (see Table I)
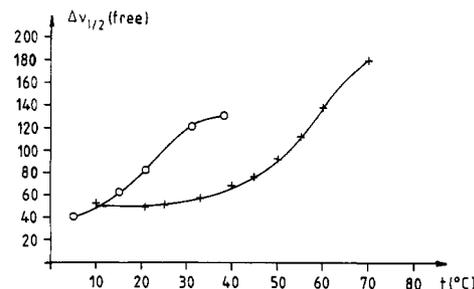
and dissociation of Ca²⁺ ions could occur by either pathway (see Figure 2). However, it should be noted that for most of the mutants studied we do see two distinct dissociation processes, and each of these has an amplitude that appears to be consistent with the loss of a single Ca²⁺ ion. An exception is (E17Q + D19N), for which the observed amplitudes and rates might result from a branched dissociation pattern such as that demonstrated for parvalbumin (Breen et al., 1985; White, 1988). Thus, it would appear that for this group of mutants the dissociation occurs predominantly via either the upper or lower pathway of Figure 1. This allows us to calculate a maximum rate constant for binding of Ca²⁺ to site I or site II when the other site is empty.

From eq 1 we note that two extreme cases are possible for the dissociation kinetics: (a) Dissociation occurs predominantly via the upper pathway with the second Ca²⁺ ion dissociating from site I. Thus, $K_I = k_{on}^I/k_{off}^I$. However, the maximum value of K_I is equal to K_1 (see eq 1, and therefore $k_{on(max)}^I = k_{off}^I K_1$. (b) By similar reasoning, for dissociation predominantly via the lower pathway we find that $k_{on(max)}^{II} = k_{off}^{II} K_1$.

Using these equations, we calculate the following values for the maximum association rate constant for binding to *either* site I or site II under conditions where the other site is unoccupied (M⁻¹ s⁻¹): 9 × 10⁸ for wild type, 2 × 10⁸ for (E17Q), 3 × 10⁸ for (D19N), 2 × 10⁸ for (E26Q), 2 × 10⁸ for (E17Q + D19N), 3 × 10⁷ for (E17Q + E26Q), 7 × 10⁷ for (D19N + E26Q), and 2 × 10⁷ for (E17Q + D19N + E26Q). For mutants with two distinct dissociation processes we use k_s as k_{off}^I (or k_{off}^{II}). When only a single exponential is seen, more than one interpretation is possible [see Forsén et al. (1988)]. The case where $k_{off}^{II,I} = k_s$ and $k_{off}^I \gg k_s$ (or $k_{off}^{I,II} = k_s$ and $k_{off}^{II} \gg k_s$ for the lower pathway) is excluded for the wild type and mutant (E17Q) on the basis of the results for the other mutants. We therefore set $k_{off}^I = 1.7k_s$ (or $k_{off}^{II} = 1.7k_s$) for these proteins. The factor of 1.7 was obtained by calculating curves for dissociation via one of the pathways only, using equations given by Breen et al. (1985), and comparing with single exponential curves. The observed rate constant is thus not equal to $k_{off}^{I,II}$ and k_{off}^{II} (or $k_{off}^{II,I}$ and k_{off}^I) but is somewhat lower. The single-exponential process observed for mutant (D19N + E26Q) is somewhat surprising, but using $1.7k_s$ for k_{off}^I (or k_{off}^{II}) nevertheless gives an upper limit for the association rate constant. Thus, it would seem that charge neutralization has resulted in a decreased association rate constant for Ca²⁺ binding to the apoprotein.

If the increase in the association rate constant for Ca²⁺ is, in fact, due to the presence of the cluster of negative surface charges, one might expect to observe a corresponding decrease in the association rate constant for the wild-type protein on increasing the ionic strength. Combining the measured values of k_s (Table II) at 0.10 M KCl with the macroscopic (stoichiometric) equilibrium constant at the same KCl concen-

tration (Table 1), using the assumptions outlined above, one obtains the following values for $k_{on(max)}^{II}$ or $k_{on(max)}^{I}$ (M^{-1} s^{-1}): 2×10^7 for wild type, 2×10^7 for (E17Q), 4×10^7 for (D19N), 2×10^7 for (E26Q), 1×10^7 for (E17Q + D19N) 1×10^7 for (E17Q + E26Q), 1×10^7 for (D19N + E26Q), and 1×10^7 for (E17Q + D19N + E26Q). Thus, in the presence of 0.1 M KCl the association rate constant for Ca^{2+} binding to the wild-type protein is significantly decreased, while the effect on the triple mutant is only slight.

By use of site-specific mutants it is evidently possible to assess contributions of individual amino acid side chains to the kinetics of Ca^{2+} association and dissociation for bovine calbindin D_{9k}. The high Ca^{2+} affinity of this protein appears to be partly due to the negative surface charges that are clustered around the Ca^{2+} binding sites [see Figure 1 and Linse et al. (1988)]. The present study demonstrates that these negative surface charges contribute to the Ca^{2+} affinity at least in part through an acceleration of the association rate constant for Ca^{2+} binding. Neutralization of three charges decreases the association rate constant for Ca^{2+} to one of the sites by about 50-fold, while the dissociation rate constant remains essentially unaltered. The most probable explanation for the high value of the apparent association rate constant is that the initial encounter (or outer-sphere) complex formed between protein and metal is strengthened by electrostatic interaction of the positively charged metal ion with these negative groups. This enhanced affinity most probably derives from a decreased rate of dissociation of the encounter complex (compared with that for the complexes formed with mutants with neutralized charges) rather than from changes in the diffusion-controlled collision rate constants for formation of this weak complex.

The modifications within the loop sequence of the pseudo EF hand were made to make this loop sequence closer in length to that of a normal EF hand. All of them lead to reduced affinity for Ca^{2+}, which is reflected in a substantial increase in the rate of Ca^{2+} dissociation from the modified site. Although the pseudo EF hand in the wild-type protein has an unusual structure, it still has a high affinity for Ca^{2+}. This suggests that the overall liganding structure must be relatively similar to that of a normal EF hand and that the inclusion of the extra two residues is compensated for by conformational adjustments in neighboring parts of the protein. It is apparent that simply removing the additional residues does not, in the case of calbindin, automatically confer a normal EF hand conformation with high Ca^{2+} affinity. The observed reduced affinity of the mutants might be due to the eliminated residues having some subsidiary but important role either in influencing the structure of the pseudo EF hand or in promoting the ability of the wild-type protein to fold into an optimally active conformation. In the case of ligand binding properties it is worth noting that even a small displacement of a liganding group could have a profound effect on binding affinity without affecting the secondary or tertiary structure significantly. Only structural studies at the highest resolution appear able to resolve this issue.

Modifications within the loop sequence of the pseudo EF hand (site 1) appear to have rather small effects on the properties of site II. This suggests that the protein can undergo the necessary local conformational adjustments associated with the deletion/substitution of one or two residues in this site without affecting tertiary structure around site II. In contrast, neutralization of some surface charge groups close to site I has a substantial effect on the properties (both kinetic and equilibrium) of site II. It seems possible that neutralization of these charges (Glu-17, Asp-19, Glu-26) reduces repulsion of negative charges (such as Glu-15 and Glu-60, see Figure 1) linked to site II. This might allow closer approach of the two sites, which would facilitate the transmission of conformational effects on Ca^{2+} binding to one of the sites.

In conclusion, our results indicate that binding free energies and kinetic properties of metal ions—and presumably also of other small charged molecules—on proteins are not determined entirely by the nature and spatial arrangement of the amino acids directly involved as ligands. The binding process involves dynamic changes in the protein structure, and protein surface charges may therefore exert a pronounced influence on the binding affinity through effects on the kinetics of ion association. Furthermore, the case of calbindin shows that deviation from the consensus sequence for the EF-hand pattern may apparently be accommodated by minor local changes in protein tertiary structure, without sacrificing binding affinity. Finally, these results show that whereas the comparison of protein structures at the level of sequence homology and identity is a powerful indicator of functional similarity, as exemplified by the family of Ca^{2+} binding proteins with the EF-hand motif, the evaluation of the contribution to affinity and kinetics of individual amino acid residues requires careful quantitation of both wild-type and selectively designed mutant proteins. The example of calbindin suggests that each protein may exhibit characteristic and specific features relating the dynamic protein structure to the binding site properties.

REFERENCES

Akke, M., & Forsén, S. (1990) *Proteins: Struct., Funct., Genet.* (in press).

Breen, P. J., Johnson, K. A., & Horrocks, W. D., Jr. (1985) *Biochemistry 24*, 4997–5004.

Brodin, P., Grundstrom, T., Hofmann, T., Drakenberg, T., Thulin, E., & Forsén, S. (1986) *Biochemistry 25*, 5371–5377.

Chazin, W. J., Kordel, C. J., Thulin, E., Hofmann, T., Drakenberg, T., & Forsén, S. (1989) *Biochemistry 28*, 8646–8653.

Clarke, D. M., Maruyama, K., Loo, T. W., Leberer, E., Inesi, G., & MacLennan, D. H. (1989) *J. Biol. Chem. 264*, 11246–11251.

Creighton, T. E. (1983) *Proteins*, p 7, Freeman, New York.

Drakenberg, T., Forsén, S., & Lilja, H. (1983) *J. Magn. Res. 53*, 412–422.

Forsén, S., Linse, S., Thulin, E., Lindegard, B., Martin, S. R., Bayley, P. M., Brodin, P., & Grundstrom, T. (1988) *Eur. J. Biochem. 177*, 47–52.

Hofmann, T., Eng, S., Drakenberg, T., Vogel, H. J., & Forsén, S. (1988) *Eur. J. Biochem. 172*, 307–313.

Johansson, C., Brodin, P., Grundstrom, T., Thulin, E., Forsén, S., & Drakenberg, T. (1990) *Eur. J. Biochem. 187*, 455–460.

Kellis, J. T., Nyberg, K., Sali, D., & Fersht, A. R. (1988) *Nature 333*, 784–786.

Knowles, J. R. (1987) *Science 236*, 1252–1258.

Kretsinger, R. H. (1987) *Cold Spring Harbor Symp. Quant. Biol. 52*, 499–510.

Kretsinger, R. H., & Nockolds, C. E. (1973) *J. Biol. Chem. 248*, 3313–3326.

Linse, S., Brodin, P., Drakenberg, T., Thulin, E., Sellers, P., Elmden, K., Grundstrom, T., & Forsén, S. (1987) *Biochemistry 26*, 6723–6735.

Linse, S., Brodin, P., Johansson, C., Thulin, E., Grundstrom, T., & Forsén, S. (1988) *Nature 335*, 651–652.

Long, J. E., Durham, B., Okamura, M., & Millet, F. (1989) *Biochemistry 28*, 6970–6974.

MacKinnon, R., Latorre, R., & Miller, C. (1989) *Biochemistry 28*, 8092–8099.

Martin, S. R., Andersson Teleman, A., Bayley, P. M., Drakenberg, T., & Forsén, S. (1985) *Eur. J. Biochem. 151*, 543–550.

Matsumura, M., Becktel, W. J., & Matthews, B. (1988) *Nature 334*, 406–410.

Perry, K. M., Onuffer, J. J., Gittelman, M. S., Barmat, L., & Matthews, C. R. (1989) *Biochemistry 28*, 7961–7968.

Rigler, R., Roslund, J., & Forsén, S. (1990) *Eur. J. Biochem.* (in press).

Sali, D., Bycroft, M., & Fersht, A. R. (1988) *Nature 335*, 740–743.

Shaw, W. V. (1987) *Biochem. J. 246*, 1–17.

Shoemaker, K. R., Kim, P. S., York, E. J., Stewart, J. M., & Baldwin, R. L. (1987) *Nature 326*, 563–567.

Szebenyi, D. M. E., & Moffat, K. (1986) *J. Biol. Chem. 261*, 8761–8777.

Thomas, P. G., Russell, A. J., & Fersht, A. R. (1985) *Nature 318*, 375–376.

Tsai, M. D., Drakenberg, T., Thulin, E., & Forsén, S. (1987) *Biochemistry 26*, 3635–3643.

Vogel, H. J., Drakenberg, T., Forsén, S., O'Neil, J. D. J., & Hofmann, T. (1985) *Biochemistry 24*, 3870–3876.

Weber, P. C., Lukas, T. J., Craig, T. A., Wilson, E., King, M. M., Kwiatkowski, A. P., & Watterson, D. M. (1989) *Proteins: Struct., Funct., Genet. 6*, 70–85.

Wendt, B., Hofmann, T., Martin, S. R., Bayley, P. M., Brodin, P., Grundstrom, T., Thulin, E., Linse, S., & Forsén, S. (1988) *Eur. J. Biochem. 175*, 439–445.

White, H. D. (1988) *Biochemistry 27*, 3357–3365.

NMR Structural Refinement of an Extrahelical Adenosine Tridecamer d(CGCAGAATTCGCG)₂ via a Hybrid Relaxation Matrix Procedure[†]

Edward P. Nikonowicz, Robert P. Meadows, and David G. Gorenstein*

Department of Chemistry, Purdue University, West Lafayette, Indiana 47907

Received September 25, 1989; Revised Manuscript Received November 20, 1989

ABSTRACT: Until very recently interproton distances from NOESY experiments have been derived solely from the two-spin approximation method. Unfortunately, even at short mixing times, there is a significant error in many of these distances. A complete relaxation matrix approach employing a matrix eigenvalue/eigenvector solution to the Bloch equations avoids the approximation of the two-spin method. We have calculated the structure of an extrahelical adenosine tridecamer oligodeoxyribonucleotide duplex, d-(CGCAGAATTCGCG)₂, by an iterative refinement approach using a hybrid relaxation matrix method combined with restrained molecular dynamics calculations. Distances from the 2D NOESY spectra have been calculated from the relaxation rate matrix which has been evaluated from a hybrid NOESY volume matrix comprising elements from the experiment and those calculated from an initial structure. The hybrid matrix derived distances have then been used in a restrained molecular dynamics procedure to obtain a new structure that better approximates the NOESY spectra. The resulting partially refined structure is then used to calculate an improved theoretical NOESY volume matrix which is once again merged with the experimental matrix until refinement is complete. Although the crystal structure of the tridecamer clearly shows the extrahelical adenosine looped out way from the duplex, the NOESY distance restrained hybrid matrix/molecular dynamics structural refinement establishes that the extrahelical adenosine stacks into the duplex.

Two-dimensional nuclear magnetic resonance (2D NMR), combined with distance geometry (Braun & Go, 1983; Havel et al., 1983; Wüthrich, 1986) or restrained molecular mechanics/dynamics (Nilsson et al., 1986), is now capable of elucidating the fine structure of short DNA strands in solution. Typically, the evaluation of interproton distances from a 2D NMR nuclear Overhauser effect spectroscopy (NOESY)

experiment depends on the so-called "two-spin approximation" (Clore & Gronenborn, 1985; Wüthrich, 1986). The approximation requires that the NOESY-derived distances be obtained from vanishingly short experimental mixing times where the buildup of NOE intensity is proportional to the inverse sixth power of the interproton distance and the effects of spin diffusion (NOE intensity mediated by multiple relaxation pathways) are minimal. Because many of the structurally important longer range NOEs are not observed at these short mixing times, the use of the two-spin approximation has raised concern over the validity of highly refined NMR structures derived by this methodology (Gorenstein et al., 1989; Keepers & James, 1984). To obtain a large number of more accurate distances, we have invoked the use of a complete relaxation